Title: Study of Anopheles gambiae 3-hydroxykynurenine transaminase activity and inhibition by LC-MS/MS method

Authors: Rossana Canavesi, Riccardo Miggiano, Martina Stella, Ubaldina Galli, Franca Rossi, Menico Rizzi, Erika Del Grosso

PII: S0731-7085(19)30073-1
DOI: https://doi.org/10.1016/j.jpba.2019.05.025
Reference: PBA 12657

To appear in: *Journal of Pharmaceutical and Biomedical Analysis*

Received date: 21 January 2019
Revised date: 8 May 2019
Accepted date: 12 May 2019

Please cite this article as: Canavesi R, Miggiano R, Stella M, Galli U, Rossi F, Rizzi M, Del Grosso E, Study of Anopheles gambiae 3-hydroxykynurenine transaminase activity and inhibition by LC-MS/MS method, *Journal of Pharmaceutical and Biomedical Analysis* (2019), https://doi.org/10.1016/j.jpba.2019.05.025

Study of Anopheles gambiae 3-hydroxykynurenine transaminase activity and inhibition by LC-MS/MS method

Rossana Canavesi, Riccardo Miggiano, Martina Stella, Ubaldina Galli, Franca Rossi, Menico Rizzi, Erika Del Grosso*

Department of Pharmaceutical Sciences, Università del Piemonte Orientale, Largo Donegani 2, 28100 Novara, Italy

*__Corresponding author__: - Department of Pharmaceutical Sciences, Università del Piemonte Orientale, Largo Donegani 2, 28100 Novara, Italy Tel: +39-0321375758; fax: +39-0321375621 e-mail address: erika.delgrosso@uniupo.it

Graphical abstract

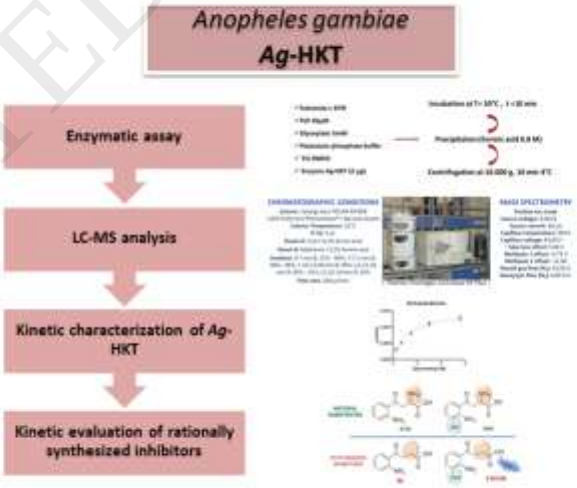

Highlights

- Enzymatic assay for the study of Anopheles gambiae 3-hydroxykynurenine transaminase
- Development and evaluation of a new LC-MS/MS
- Kinetic characterization of Ag-HKT with the new method
- Applicability of the new LC-MS/MS method for the kinetic evaluation of rationally synthesized inhibitors

Abstract

In *Anopheles gambiae*, the most efficient vector of the malaria parasite *Plasmodium falciparum*, 3-hydroxykynurenine is endowed with a toxic potential. In adult mosquitoes, the excess of 3-hydroxykynurenine is removed by a specific transaminase (3-hydroxykynurenine transaminase, HKT) which converts the compound into the more stable xanthurenic acid. Interfering with 3-hydroxykynurenine metabolism in *A. gambiae* is a potential approach for the development of transmission-blocking drugs and insecticides. Hence, the aims of this work were to develop and validate a new LC-MS/MS method for the evaluation of *A. gambiae* 3-hydroxykynurenine transaminase (*Ag*-HKT) activity and the determination of the potency of inhibitors of the enzyme. We set up a LC-MS/MS-based enzymatic assay for the determination of kinetic constants values of the recombinant *Ag*-HKT enzyme and for the evaluation of *Ag*-HKT inhibition by a known protein inhibitor used as reference and a newly synthesized compound. The chromatographic separation was performed in a gradient mode on a Phenomenex Synergi Polar-RP (150 x 2.0, 4 µm) with methanol and water containing both 0.2% formic acid. Mass spectrometric detection was achieved with an ion trap equipped with an ESI source, in positive ionization scan, operating in SRM mode. The LC-MS/MS method was validated in terms of selectivity, linearity, precision and accuracy.

Abbreviations

***Ag*-HKT:** *A. gambiae* 3-hydroxykynurenine transaminase

KP: kynurenine pathway

3-HK: L-3-hydroxykynurenine

XA: xanthurenic acid

KYN: kynurenine

KA: kynurenic acid

INI: 4-(2-aminophenyl)-4-oxobutanoic acid

3-OH-INI: 4-(2-Amino-3-hydroxyphenyl)-4-oxobutanoic acid

Keywords: LC-MS/MS, *Ag*-HKT, *Anopheles gambiae*, kynurenine pathway, enzyme assay

1. Introduction

Malaria is a vector-borne disease that is caused by apicomplexan parasites belonging to the *genus Plasmodium*, including the *Plasmodium falciparum* species, which is the predominant etiological agent of both uncomplicated and severe malaria cases in humans [1]. The *P. falciparum* natural infection is efficiently spread through the human population by the bite of parasite-infected female anopheline mosquitoes, mainly by members of the *Anopheles gambiae* complex, which therefore represent the deadliest malaria vectors world-wide [2]. In spite of the recent success in reducing the malaria global burden and the advances in the development of an effective malaria vaccine (RTS,S) [3], there is still an urgent need for novel approaches to fight the alarming emergence of *Plasmodium* strains that gained resistance to all of the currently available anti-malarial drugs, and to contain the expansion of insecticide-resistant *Anopheles* mosquito populations [4,5]. In this scenario, the molecular study of central metabolic pathways, such as the kynurenine pathway (KP) for the oxidative degradation of tryptophan, could provide useful information for the identification

of potential targets of innovative insecticides and malaria transmission-blocking drugs. In all animal species examined thus far, most of the metabolites produced along the KP (Fig. 1) behave as bioactive compounds, playing central roles in fundamental aspects of the organism biology. In insects, the actions of KP metabolites range from acting as substrates for eggs, body and eye pigments synthesis [6], to triggering tissue remodelling during metamorphosis [7], to modulating complex behaviours [8]. Within the KP, L-3-hydroxykynurenine (3-HK) is endowed with a toxic potential, due to spontaneous oxidation that produces reactive oxygen species displaying cytotoxic and pro-apoptotic properties [7,9].

In mammals 3-HK could be metabolized by two main routes: i) by direct transformation into xanthurenic acid (XA), through an irreversible transamination reaction catalysed by a limited number of pyridoxal-5'-phosphate (PLP)-dependent aminotransferases (collectively indicated as kynurenine aminotransferases or KATs); or ii) by kynureninase-dependent hydrolysis, that yields 3-hydroxyanthranilic acid, which is fluxed in the main branch of the KP, leading to the *de novo* nicotinamide adenine dinucleotide (NAD) synthesis [10]. In insects, this latter mechanism is precluded by the absence of a kynureninase function. Consequently, the 3-HK aminotransferase (3-HKT)-dependent conversion of 3-HK to XA is needed to contrast the harmful accumulation of 3-HK exceeding the ommochrome synthesis requirements [11]. XA plays multiple roles in the physiology of mosquitoes that are vectors of human diseases [reviewed in 11]. In particular, XA is reported as a main *heme*-iron chelator, therefore contributing to neutralize the pro-oxidant potential associated to the insect hematophagous behaviour [12]. Moreover, mosquito-synthesized XA is a trigger of the *Plasmodium* "exflagellation", a spectacular phenomenon that brings the parasite male gametes to full maturation, and that takes place in the midgut of the female mosquito, upon a parasite-infected blood meal [13]. For these reasons, the unbalance of XA homeostasis, through the inhibition of enzymes in the KP -and of 3-HKT in particular-, can be considered a promising approach to impact the mosquito vector physiology *per se*, and the capability of the *Plasmodium*-infected female individuals to sustain optimal parasite replication. Two main *in vivo* observations

corroborate this hypothesis. The siRNA-mediated silencing of the 3-HKT coding gene in *Anopheles stephensi* larvae -which has been obtained by feeding the mosquito larval stages with transgenic microalgae-, results in their impaired development or death [14]. In addition, *Plasmodium berghei* oocysts formation is severely inhibited in the midgut of a XA-deficient *Anopheles stephensi* strain, which has been obtained by knocking-out the kynurenine 3-monooxygenase gene, leading to a reduced number of sporozoites in the mosquito salivary glands [15]. Although very promising, these genetics approaches are extremely challenging, and the pursuing of innovative small-molecule insecticides to fight the mosquito vectors of human pathogens still represent a research priority.

The determination of the crystal structures of *Anopheles gambiae* 3-HKT (*Ag*-HKT) both in its PLP-bound form, and in complex with an inhibitor that mimics the kynurenine (KYN) substrate, but lacks the α-amino group (compound **INI** in Fig. 2a) [16], allowed the description of the enzyme molecular determinants involved in substrate recognition and binding. Of outmost interest, a class of isoxazoles [17] and 1,2,4-oxadiazoles [18], which display potent activity *in vivo* against the dengue vector *Aedes aegypti* larvae, have been developed, also basing on molecular docking experiments using the *Ag*-HKT:INI complex atomic coordinates as the template, therefore pointing to *Ag*-HKT as a possible target.

The current efforts aimed at the selection and/or the structure-based rational design of *Ag*-HKT-specific inhibitors should be paralleled by analytical methods able to evaluate any potential candidate in terms of potency, affinity and mechanism of action. Several analytical techniques, such as liquid chromatography (LC) coupled with ultraviolet (UV), electrochemical (EC), or mass spectrometry (MS) detectors, have been applied to quantify tryptophan and its metabolites in various biological matrix [19-21]. To date, an HPLC-ECD method was reported for the determination of 3-HK and XA levels in *A. aegypti* and *D. melanogaster* larvae extracts, as well as to detect 3-HK transaminase activities [22]. Furthermore, an HPLC-UV method was adopted for the kinetic characterization of the *A. gambiae* 3HKT [23], and the *Aedes aegypti* functionally equivalent enzyme [24], towards substrates as D,L-3-HK, D,L-KYN and L-KYN.

In the present work, a new selective and specific LC-MS/MS method was developed and validated with the aim of studying new potential inhibitors of the enzyme, using the recombinant *Ag*-HKT enzyme and L-KYN and KA for the LC-MS/MS quantification method. The method was validated for selectivity, linearity, precision, and accuracy. A further advantage of the LC-MS/MS-based approach is represented by the direct measurement of substrates and products with greater sensitivity and selectivity. The robustness and reliability of the method for its future use in screening procedures for the identification of potent and selective Ag-HKT inhibitors, was evaluated in the analysis of a newly synthesized compound (**3-OH-INI,** Fig. 2b), which differs from the previously described **INI** molecule (Fig. 2a, see above) for the presence of a hydroxyl group at position 3 of the anthranilic ring, therefore more closely mimicking the 3-HK physiologic substrate, and in principle better exploiting the ligand binding potential of the *Ag*-HKT ligand binding cavity with respect to **INI** [16].

2. Experimental

2.1 Materials and methods

Methanol (HPLC grade), formic acid, L-kynurenine (MW 208.21; L-KYN), kynurenic acid (MW 189.2 ; KA), xanthurenic acid (MW 205.17 ; XA), 3-hydroxy-DL-kynurenine (MW 224.21 ; D,L-3-HK), pyridoxal 5′-phosphate (PLP), sodium glyoxylate monohydrate, dimethyl sulfoxide (DMSO) were supplied by Sigma-Aldrich (St. Louis, MO, USA). Water (HPLC grade) was obtained from Milli-Q reverse osmosis system (Millipore Co., Billerica MA, USA). Petroleum ether (PE), ethyl acetate (EtOAc), glacial acetic acid (AcOH), ethanol (EtOH), dichloromethane (DCM) and commercially available reagents were purchased from Aldrich or Alfa Aesar, and were used without further purification. 4-(2-aminophenyl)-4-oxobutanoic acid (**INI**) was kindly gifted by CAGE Chemicals (Novara, Italy). Flash column chromatography was performed on silica gel (Merck Kieselgel 60, 230–400 mesh ASTM). Thin layer chromatography (TLC) was carried out on 5x10 cm plates with a layer thickness of 0.25 mm (Merck Silica gel 60 F254); when necessary, they were

developed with $KMnO_4$ reagent. The recombinant Ag-HKT enzyme was expressed and purified as previously described [23].

2.2 Spectroscopic analyses and chemical characterization

Melting points were determined in open glass capillary with a Stuart scientific SMP3 apparatus and are uncorrected. All compounds were checked by IR (FT-IR THERMO-NICOLET AVATAR), ^{1}H and ^{13}C APT (JEOL ECP 300 MHz spectrometer), and mass spectrometry (Thermo Finningan LCQ-deca XP-plus), equipped with an ESI source and an ion trap detector.

2.3 Instrumentation and chromatographic conditions

2.3.1 LC-MS/MS analyses

A Thermo Finningan LCQ Deca XP Plus ion trap mass spectrometer equipped with a quaternary pump, a Surveyor AS autosampler and a vacuum degasser was used for LC-MS analysis (Thermo Electron Corporation, Waltham, MA, USA). The chromatographic separation was performed using a Phenomenex Synergi™ 4 µm Polar-RP 80 Å (150 x 2.0 mm I.D) column with a Polar SecurityGuard column (Phenomenex, Torrance, CA, USA) maintained at 25 °C. The injection volume was 5 µl. A mobile phase (flow rate 200 µl/min) was used consisting of water with 0.2% formic acid (solvent A) and methanol with 0.2% formic acid (solvent B). A gradient elution was set as follows: 25-90% solvent B in 7 min, up to 95% solvent B in 0.1 min, held at 95% solvent B for 5.0 min, then column reconditioning at 25% solvent B to 18 min. The eluate was injected into the electrospray ion source between 2.0 and 17.90 minutes whereas the eluate was sent to waste before and after the run time. The operating conditions of the mass spectrometer in positive mode were the following: source voltage, 4.00 kV; source current, 80 µA; capillary temperature, 350 °C; capillary voltage, 44.00 V; tube lens offset, 5.00 V; multipole 1 offset, -4.75 V; multipole 2 offset, -11.00 V; sheath gas flow (N_2) 45,00 AU; sweep gas flow 4,00 AU. Data were acquired both in selected reaction monitoring (SRM) and in full-scan in electrospray positive ion mode. The SRM transitions

and the corresponding collision energies (CE) were as follow: L-KYN (*m/z* 209 → *m/z* 192; CE = 20%), KA (*m/z* 190 → *m/z* 172; CE = 35%), D,L-3-HK (*m/z* 225 → *m/z* 208 ; CE = 20%), XA (*m/z* 206 → *m/z* 188 ; CE = 35%). The acquisition in full scan was performed using mass scan range *m/z* 50 to 500. MS spectra were acquired and processed using Xcalibur® software (Thermo Fisher Scientific)

2.3.2 Synthesis of novel inhibitor 3-OH-INI

*2.3.2.1 3ˈ-Hydroxy-2ˈ-nitroacetophenone (**2**)*

To a solution of 3-hydroxyacetophenone (**1**) (15.00 g, 0.1103 mol) in EtOAc (230 mL) was slowly added nitric acid 90% v/v (8.0 mL) at 0 °C and the mixture was stirred at room temperature overnight. The reaction was monitored by TLC with PE/EtOAc 8:2 (R_f 0.22), then the mixture was diluted with EtOAc and washed successively with water (x1), sat. aq. $NaHCO_3$ (x1) and brine (x1). The organic layer was dried over Na_2SO_4 and concentrated under reduced pressure. The crude product was purified by two sequential column chromatography using DCM followed by PE/EtOAc 9:1 and PE/EtOAc 5:5 as eluents to give 5.0 g of product as a pale yellow solid, yield 25%. The compound was crystallized with EtOH/PE to afford an off white solid, mp 137-138 °C, (lit. [25] 131-132 °C; lit. [26] 134-136 °C); IR (KBr) 3142-2710 (br), 1668, 1583, 1532, 1473, 1376, 1292, 799 cm $^{-1}$; ^{1}H-NMR (300 MHz, $CDCl_3$) δ 10.51 (s, 1-H), 7.59 (t, J = 7.6 Hz, 1-H), 7.21 (dd, J = 8.2/1.2 Hz, 1-H), 6.83 (dd, J = 7.3/1.2 Hz, 1-H), 2.51 (s, 3-H) ppm; ^{13}C-NMR (75 MHz, $CDCl_3$) δ 199.6, 155.3, 140.8 (2-C), 137.1, 121.3, 118.3, 30.5 ppm. MS (ESI) *m/z* 180 $(M-H)^-$.

*(E)-4-(3-Hydroxy-2-nitrophenyl)-4-oxobut-2-enoic acid (**3**)*

A mixture of 3ˈ-Hydroxy-2ˈ-nitroacetophenone (**2**) (2.10 g, 11.60 mmol, 1 equiv) and glyoxylic acid monohydrate (1.07 g, 11.60 mmol, 1 equiv) in 20 mL glacial acetic acid and 2 mL conc. HCl was heated under reflux. After 5 h glyoxylic acid monohydrate (1.07 g, 11.60 mmol, 1 equiv) was added and the mixture was further heated under reflux overnight. The reaction progress was monitored by TLC with PE/EtOAc 5:5 + 1% AcOH, (R_f 0.3). The solvents were removed under

reduced pressure and the residue was purified by column chromatography using DCM + 1% AcOH and successively PE/EtOAc 7:3 + 1% AcOH as eluants to give 1.0 g of product as a yellow solid, yield 36%, mp 159-160 °C (lit. [25] 158 °C; lit. [26] 158-159 °C); IR (KBr) 3296-2521 (br), 1704, 1677, 1602, 1519, 1432, 1274, 1169, 977 cm $^{-1}$; ^{1}H-NMR (300 MHz, CD_3OD) δ 7.54 (t, J = 8.3 Hz, 1-H), 7.43 (dd, J = 15.9/0.9 Hz, 1-H), 7.26 (d, J = 8.3/0.9 Hz, 1-H) ppm; ^{13}C-NMR (75 MHz, CD_3OD) δ 191.3, 167.9, 152.7, 138.9, 138.0, 135.1, 134.4, 134.0, 123.1, 121.1 ppm. MS (ESI) *m/z* 238 $(M+H)^+$.

*2.3.2.2 4-(2-Amino-3-hydroxyphenyl)-4-oxobutanoic acid (**3-OH-INI**)*

To a solution of (*E*)-4-(3-Hydroxy-2-nitrophenyl)-4-oxobut-2-enoic acid (**3**) (0.61 g, 2.58 mmol, 1 equiv) in EtOAc (62 mL) and AcOH (1 mL, 18.07 mmol, 7 equiv) Pd/C 5% (95 mg) was added as catalyst. The mixture was stirred under hydrogen atmosphere (1 atm) at 25 °C in the dark for 18 h. The reaction progress was monitored by TLC with PE/EtOAc 5:5 + 1% AcOH, (R_f 0.42). The resulting suspension was filtered through a pad of Celite and the solvent was removed *in vacuo*. The residue was purified by column chromatography using PE/ EtOAc 7:3 + 1% AcOH as eluant to give 0.25 g of product as a light brown solid, yield 46%, mp 134-135 °C (lit. [26] 134-135 °C); IR (KBr) 3504, 3382, 3278, 2929, 1717, 1677, 1643, 1543, 1273, 1175, 739 cm $^{-1}$; ^{1}H-NMR (300 MHz, CD_3OD) δ 7.35 (d, J = 8.2 Hz, 1-H), 6.79 (d, J = 7.6 Hz, 1-H), 6.46 (t, J = 8.0 Hz, 1-H), 3.24 (t, J = 6.4 Hz, 2-H), 2.64 (t, J = 6.4 Hz, 2-H) ppm; ^{13}C-NMR (75 MHz, CD_3OD) δ 201.9, 177.1, 146.2, 142.0, 122.5, 118.8, 117.8, 115.6, 35.0, 29.2 ppm. MS (ESI) *m/z* 210 $(M+H)^+$.

2.4 Preparation of solutions

Stock solutions were prepared by dissolving KA in MeOH to achieve a final concentration of 500 µM. Working solutions of KA were prepared by diluting stock solutions in a solvent mixture constituted by 50% of water with 0.2% formic acid (solvent A) and 50% of methanol with 0.2% formic acid (solvent B) to reach the appropriate concentrations. IS stock solution was prepared in buffer phosphate (200 mM, pH 7.0) at 2 mM and then diluted to 10 µM with (solvent A)/ (solvent

B) 50/50 *v/v* to obtain the corresponding working solution. Working solutions obtained were used for the preparation of matrix-based calibration standards, quality control, blank and zero samples. Calibration standards (final volume, 1 mL) were prepared by diluting appropriate volumes of KA working solutions in the presence of 10 µL of matrix obtaining eight calibration standards for KA at concentration ranging from 0.25 to 50 µM in the presence of IS (XA 2.5µM). A mixture of all components involved in the enzymatic assay constitutes the matrix (i.e. DMSO; *Ag*-HKT 0.4 µg/µL; buffer phosphate 200 mM, pH 7.0; formic acid 0.8 M: the matrix was vortexed, centrifuged at 12.000 rpm for 5 min: under these conditions, the enzyme is inactive). Quality controls (QC) samples were prepared from a separate stock solution in the same way as the calibration standards. Blank samples were prepared in the mobile phase containing the matrix without the IS. Zero samples were obtained by adding the IS to the mobile phase containing the matrix.

2.5 LC-MS/MS method validation

The LC-MS/MS method was validated in terms of selectivity, linearity, accuracy, precision, recovery, matrix effect and stability. Selectivity was assessed by the analysis of blank enzymatic assay mixture (a), blank enzymatic assay mixture spiked with standard compounds (b), enzymatic assay mixture after reaction (c). Extracted ion chromatograms for each analyte were used to evaluate the presence of potential interfering substances at the corresponding retention time. Linearity was determined for KA at eight concentrations levels ranging from 0.25 µM to 50 µM, in the presence of IS used at the fixed concentration of 2.5 µM. Calibration of the method was performed by using standards prepared as described above on three non-consecutive days. The peak-area ratio between the analyte and internal standard was used after quantitative integration by Xcalibur® software. The calibration curves were obtained by plotting the peak-area ratio with the analyte concentration of the standard KA using 1/x weighted linear regression. Moreover, LLOQ was determined on signal-to-noise ratio by establishing the minimum concentration at which the

analyte is characterized to have at least a signal to noise ratio of 5:1 compared to blank response. Accuracy and precision of the analytical method were measured for QC samples at four concentration levels containing known amounts of the analyte, by repeating five times the analysis per concentration. The mean value should be within 15% of the actual value except at LLOQ, where it should not deviate by more than 20%. Intra-batch and inter-batch precisions were determined by using the relative standard deviation (RSD %) of the replicate samples between three non-consecutive days. The precision determined at each concentration level should not exceed 15% of the RSD except for the LLOQ, where it should not exceed 20% of the RSD. The matrix effect was determined at low, medium, and high concentrations in triplicates by comparing the response of the analyte spiked in extracted matrix with the response of analyte obtained from solvent solutions. Recovery was calculated at the same concentrations by comparing the response of extracted QC samples with the extracted matrix spiked with the analyte. The stability assay was performed by analyzing QC samples after storage at room temperature for 12 h.

2.6 Ag-HKT activity assay

The activity of *Ag*-HKT was assessed by quantitatively determining the KA production, using L-KYN as the amino group donor and glyoxylate as the amino group acceptor in the transamination reaction, according to the published procedure with minor modifications [23]. In details, the standard incubation mixture (50 µl final volume) was assembled in 200 mM potassium phosphate buffer (pH 7.0) containing 40 µM PLP, 5 mM glyoxylate, 1.5 mM L-KYN. Reactions were initiated by the addition of 4 µg of *Ag*-HKT. The solutions were then shaken for 10 minutes at 50 °C in a Thermomixer equipment (Eppendorf, Milan, Italy). Blank incubations were carried out by omitting either the PLP co-factor, or the substrate or the *Ag*-HKT enzyme in the reaction mixtures assembling. Each incubation was stopped by adding 45 µl of formic acid (0.8 M) and 5 µL of IS solution (2 mM), vortexed and centrifuged at 13,000 rpm for 10 min. The supernatants (15 µL) were diluted in the mobile solvent (585 µl) and analysed by LC-MS/MS. In order to ensure

reproducibility, all assays were performed in duplicate and analysed twice. The protocol described above was used to determine the kinetic constants (K_M and Vmax) of the *Ag*-HKT-dependent L-KYN to KA transamination reaction, by measuring the formation of KA in the presence of L-KYN at a concentration ranging from 0.3 to 5.6 mM, followed by fitting the experimental data to the Michaelis-Menten equation (eq 1) using GraphPad Prism software 5.0 (GraphPad Software Inc., San Diego, CA)

(1) $v = \frac{V_{max} \times [S]}{K_M + [S]}$

where v is the velocity of the transamination reaction (µmol/min), Vmax is the maximal velocity (µmol/min), and K_M is the Michaelis-Menten constant (mM), [S] is the substrate concentration (mM).

2.7 Ag-HKT inhibition studies

Stock 15 mM solutions of **INI** and **3-OH-INI** were prepared in DMSO, and were tested at three different concentration (150, 300 and 750 µM) in the presence of fixed concentration of L-KYN. The DMSO final concentration in the control assays -*i.e.* in the absence of the inhibitor- has been kept at 10%. All the assays were performed following the procedure reported in the paragraph "*Ag*-HKT activity assay". After analysis in LC-MS/MS and quantitative integration by the Xcalibur® software, data have been input in a Microsoft Excel® spreadsheet. The percentage of inhibition value was calculated by using the formula [100-(CI/C0 *100)] where CI and C0 are the mean concentration of KA formed in the presence or in the absence of inhibitor, respectively.

2.8 Determination of inhibition constants (Ki) and inhibitors mechanism of action by LC-MS/MS

The Ki were determined for both **INI** and **3-OH-INI** by performing the activity assays in the presence of increasing concentrations of inhibitor (ranging from 0.06 to 1.5 mM) in the presence of L-KYN at concentration between 0.3 to 5.6 mM. Reaction rates were calculated with respect to the

calibration curve. The values obtained (expressed as µmol min-1) were used to calculated the Ki value, by plotting the inhibitor concentration (mM) to the substrate concentrations (mM), by using GraphPad Prism and Sigma Plot software. Inhibition constants for compounds **INI** and **3-OH-INI** were calculated by fitting the data to competitive inhibition equation (eq. 2)

(2) $Ki = \frac{K_M \times [I]}{K_{M\ app} - K_M}$

where Ki is the dissociation constant for the inhibitor-enzyme complex, K_M is the Michaelis-Menten constant, [I] is the inhibitor concentration in mM, and $K_{M\ app}$ is the apparent K_M value.

3. Results and discussion

3.1 LC-MS/MS method

At present, a general limit to analytical procedures based on 3-HK as the amino-group donor substrate in transamination reactions is that pure L-3-HK (the natural substrate) is not commercially available. Therefore, the published *Ag*-HKT enzyme kinetics characterization has been performed by comparing different substrates, highlighting that *Ag*-HKT displays comparable affinity and catalytic efficiency both for the the racemic mixture of D,L-3-HK and for the L-KYN substrate [23]. Moreover, D,L-3HK shows poor solubility in the reaction buffers, as previuosly described by Li et al. [22], and high instability [27], making its use not suitable for routinely screening of *Ag*-HKT inhibitors. Therefore, since the *Ag*-HKT enzyme can use also L-KYN as the amino-donor substrate with comparable efficiency, we developed a method for measuring the levels of the transamination product KA.

In the development of the LC-MS/MS method for the analysis of L-KYN and KA, the structural relationship between KA and XA was exploited in the optimization of the LC-MS/MS procedure, as XA was used as the internal standard, although deuterated standard are usually preferred.

XA was chosen as internal standard because the 8-OH in the XA structure can be exploited on the one hand for the chromatographic separation due to the similar interaction to KA with the stationary phase, and on the other hand for the similar ionization and fragmentation pattern, as shown in Supplemental 1. The chromatographic separation of analytes was achieved on a Synergy Polar column allowing the use of a simple mobile phase. The gradient elution was optimized to achieve the elution of analytes within 8 minutes of the gradient. Retention times of L-KYN, KA and IS were 3.94, 7.11 and 6.82 minutes respectively as reported in Fig. 3.

KYN, KA and IS were ionized in ESI positive mode to generate protonated molecular ions $[M+H]^+$ at *m/z* 209, 190, 206 respectively. When MS/MS experiments were performed on these ions the product ions obtained (*m/z* 192, 172 and 188 respectively) were directly used as specific transitions to increase specificity and detection responses; finally, the detection was operated in selected reaction monitoring mode (SRM). It is worth of mention that the analytical method was suitable also for the analysis of D,L-3HK compound that could be monitored following SRM transition at *m/z* 225→208 and retention time of 3.16 min, ensuring the chromatographic separation of all analytes, as shown in Supplemental 2. This evidence suggest that the method could be applied for the analysis of enzyme assay performed on 3-HK, depending on the availability of pure isomers.

3.2 LC-MS/MS validation

The selectivity of the LC-MS/MS method was assessed by analysing the blank samples, prepared as reported in the experimental part. Extracted ion chromatograms for each analyte ruled out the presence of interferences at the corresponding retention time. The representative SRM chromatograms are shown in Supplemental 3. The calibration curves obtained from analyte/IS peak area ratios versus the nominal concentration were linear using weighted (1/*x*) regression over the concentration range, with correlation coefficient $R^2 \geq 0.99$. The calibration equations were as follows: $y = 0.4042x - 0.02271$ ($R^2 = 0.9982$); $y = 0.3261x + 0.005754$ ($R^2 = 0.9974$); $y = 0.3619x + 0.001683$ ($R^2 = 0.9988$). The lower limit of quantification (LLOQ) was determined by injecting

lower concentration solutions of KA. The LLOQ value was 0.25 μM, and the representative chromatogram is reported in the Supplemental 4. Accuracy and precision were determined by measuring four concentration levels (LLOQ, low, medium and high concentration), covering the entire range of the calibration curve (data are provided in Table 1). The accuracy was between 88.21 and 111.21%. The mean intra-assay precision was below 14% and below 11% for the inter-assay precision for LLOQ, the values of intra-assay and inter-assay precision for the remaining levels were below 10.5% and 9.5% respectively. The matrix effect values were found to vary between 105% and 111% suggesting a negligible effect to ion suppression or enhancement caused by co-eluting compounds. Recovery values were found at 110%, 104% and 101% at low, medium and high concentration respectively. Stability of the standard solutions of KA and IS were studied at the benchtop at room temperature over 12 h. The concentrations of freshly prepared solutions and those aged for 12 h were determined and the difference between them was found to be not significant (RSD < 2 %). The results obtained proved that the samples solutions were stable for the specified duration.

3.3 3-OH-INI Synthesis

4-(2-Amino-3-hydroxyphenyl)-4-oxobutanoic acid **(3-OH-INI)** was prepared in a three-step synthesis starting from the commercially available 3-hydroxyacetophenone (**1**), as shown in Fig. 2b. Nitration of 3-hydroxyacetophenone (**1**) was directly carried out with HNO_3 in ethyl acetate at 25 °C to give 3ˈ-hydroxy-2ˈ-nitroacetophenone (**2**) in 25% yield. Methyl ketone **2** was condensed with 2 equiv of glyoxylic acid monohydrate in glacial acetic acid and conc. HCl under reflux for 12 h to afford (*E*)-4-(3-hydroxy-2-nitrophenyl)-4-oxobut-2-enoic acid (**3**) in 36% yield. Our synthetic procedure is easier to set up than previously reported Mizdrak's method [26] which required the use of 11.8 equiv of glyoxylic acid monohydrate and heating at 120 °C without solvent, under vacuum for 24 h. Finally, hydrogenation of **3** in ethyl acetate with glacial acetic acid, catalysed by Pd/C, afforded **3-OH-INI** in 46% yield. Acetic acid was used to assist protonation of the amino group in order to prevent the formation of Michael adduct.

3.4 Ag-HKT activity assay

Previous works demonstrated that the recombinant form of *Ag*-HKT displays comparable affinity and catalytic efficiency towards both D,L-3-HK and L-KYN, in the PLP-dependent transamination to XA and KA, respectively, by using the α-ketoacid glyoxylate as the amino group acceptor [23]. The new LC-MS-based analytical method was therefore used to quantify the KA produced in standard *Ag*-HKT activity assays for the determination of the enzyme kinetics. The calculated K_M value (1.4 ± 0.18 mM) for the *Ag*-HKT catalyzed transamination of L-KYN to KA is in agreement with the one reported in literature (1.0 ± 0.4 mM) [23].

By slightly modifying the published procedure, DMSO was added to the incubation mixtures in order to ensure the solubility of the tested inhibitors. The influence of DMSO on the enzyme activity was evaluated in the 1% to 20% v/v concentration range (data not shown). The presence of DMSO at 10% final concentration did not affect the product formation, allowing us to test inhibitors at a wide range of concentrations while keeping the compounds soluble. Moreover, the linearity of KA production was investigated and the optimal incubation time was found at 10 minutes. This evidence demonstrated the good reliability of the enzyme assay coupled to the LC-MS/MS analytical method, and its exploitability for the *in vitro* analysis of *Ag*-HKT inhibition.

The method was applied for the analysis of **3-OH-INI**, a newly synthesized compound (Fig. 2) which is different from **INI** for the presence of a hydroxyl group at position 3 of the anthranilic group; therefore, by more closely mimicking the 3-HK physiologic substrate compared to **INI**, **3-OH-INI** could represent a more efficient inhibitor of the *Ag*-HKT enzyme. Interestingly, the manual modelling of **3-OH-INI** inside the ligand binding cavity of the crystal structure of the *Ag*-HKT:INI complex [16], revealed that the 3-OH group of the modelled molecule occupies an ideal position to established a strong hydrogen bond with the side chain oxygen atom of a serine residue (Ser43) (Supplemental figure 5), which is also involved in the coordination of the amino group of

the phenyl ring of the ligand. Such an analysis suggested that **3-OH-INI** could behave as a more potent *Ag*-HKT inhibitor when compared to **INI**.

Preliminary *Ag*-HKT inhibition assays were performed by using **3-OH-INI**, or the known reference molecule **INI**, at three fixed concentrations. The obtained data revealed that the inhibitory potency of **3-OH-INI** is higher than the one of **INI** at all the concentrations studied and it was considered worthy of further investigation. Based on the results of the activity assays/LC-MS/MS analyses described above, we determined the Ki value of **INI** and **3-OH-INI** towards the L-KYN to KA transamination reaction. The Ki in the high micromolar range revealed for **INI** (740 µM) is in agreement with what has been previously reported (300 µM) [16], confirming the accuracy and the reliability of the LC-MS/MS developed procedure. Noticeably, the lowering of the Ki value revealed for **3-OH-INI** (325 µM), highlighted that the addition of the hydroxyl-group at position 3 of the **INI** reference molecule improves its potency, in line with what has been hypothesized on the basis of *Ag*-HKT structural analyses [16]. As expected, the Lineaweaver-Burk reciprocal plot analysis of the inhibition assays results (Fig. 4) indicates that **3-OH-INI** acts as a competitive inhibitor of the *Ag*-HKT enzyme.

4. Conclusion

In this work, a new LC-MS/MS method was developed and its applicability was confirmed by the determination of the kinetic constants of the *Ag*-HKT-catalysed transamination of L-KYN to KA, and the re-evaluation of **INI**, a previously describe weak inhibitor of the enzyme. Moreover, a new compound **3-OH-INI** was synthesized and analysed, showing an improved inhibition potency. The greater specificity and sensibility of the LC-MS/MS method over conventional HPLC-UV methods suggests that it can be applied for the screening of further and potential *Ag*-HKT inhibitors, also including new compounds that should be rationally designed based on the **3-OH-INI** scaffold.

Acknowledgments and Foundings

This research is original and it has been supported by Fondazione Cariplo (grant n° 2015-2246) and by University of Piemonte Orientale (grants: RSdelgrossoeRL15_ANOPHELES_GAMBIAE_16-18 and RIVrossifRL16_TRIPTOFANO_17-19).

Conflict of interest

The authors declare that they have no conflict of interest.

References

[1] Phillips M.A., Burrows J.N., Manyando C., van Huijsduijnen R.H., Van Voorhis W.C., Wells T.N.C., Malaria, Nat. Rev. Dis. Primers. 3 (2017) 1-24 https://doi.org/10.1038/nrdp.2017.50

[2] Hyde J.E. Drug-resistant malaria - an insight, FEBS J. 274 (2007) 4688-4698. https://doi.org/10.1111/j.1742-4658.2007.05999.x

[3] White N.J., Pukrittayakamee S., Hien T.T., Faiz M.A., Mokuolu O.A., Dondorp A.M., Malaria, Lancet 383 (2014) 723-35. https://doi.org/10.1016/S0140-6736(13)60024-0

[4] WHO World malaria report, 2017, http://www.who.int/malaria/publications/world-malaria-report-2017/report/en/

[5] Coleman M., Hemingway J., Gleave K.A., Wiebe A., Gething P.W., Moyes C.L., Developing global maps of insecticide resistance risk to improve vector control, Malaria J. 16 (2017) 85-95. https://doi.org/10.1016/S0140-6736(13)60024-0

[6] Figon F., Casas J. (2018). Ommochromes in invertebrates: biochemistry and cell biology, Biol. Rev. Camb. Philos. Soc., https://doi.org/10.1111/brv.12441 [Epub ahead of print]

[7] Cerstiaens A., Huybrechts J., Kotanen S., Lebeau I., Meylaers K., De Loof A., Schoofs L., Neurotoxic and neurobehavioral effects of kynurenines in adult insects, Biochem. Biophys. Res. Commun. 312 (2003) 1171–1177 https://doi.org/10.1016/j.jinsphys.2006.09.004

[8] Savvateeva E., Kynurenines in the regulation of behaviour in insects, Adv. Exp. Med. Biol. 294 (1991) 319–328

[9] Okuda S., Nishiyama N., Saito H., Katsuki H., 3-Hydroxykynurenine, an endogenous oxidative stress generator, causes neuronal cell death with apoptotic features and region selectivity, J. Neurochem. 70 (1998) 299–307 https://doi.org/10.1046/j.1471-4159.1998.70010299.x

[10] Sathyasaikumar K.V., Tararina M., Wu H.Q., Neale S.A., Weisz F., Salt T.E., Schwarcz R., Xanthurenic Acid Formation from 3-Hydroxykynurenine in the Mammalian Brain: Neurochemical Characterization and Physiological Effects, Neuroscience, 367 (2017) 85-97 https://doi.org/10.1016/j.neuroscience.2017.10.006

[11] Han Q., Beerntsen B.T., Li J., The tryptophan oxidation pathway in mosquitoes with emphasis on xanthurenic acid biosynthesis, J. Insect. Physiol. 53 (2007) 254–263 https://doi.org/10.1016/j.jinsphys.2006.09.004

[12] Lima V.L.A, Dias F., Nunes R.D., Pereira L.O., Santos T.S.R., Chiarini L.B., Ramos T.D., Silva-Mendes B.J., Perales J., Valente R.H., Oliveira P.L., The Antioxidant Role of Xanthurenic Acid in the *Aedes aegypti* Midgut during Digestion of a Blood Meal, PloS ONE 7 (2012) e38349 https://doi.org/10.1371/journal.pone.0038349

[13] Billker O., Lindo V., Panico M., Etienne A. E., Paxton T., Dell A., Rogers M., Sinden R. E., Morris H. R., Identification of xanthurenic acid as the putative inducer of malaria development in the mosquito, Nature 392 (1998) 289–292 https://doi.org/10.1038/32667

[14] Kumar A., Wang S., Ou R., Samrakandi M., Beerntsen B.T., Sayre R.T., Development of an RNAi based microalgal larvicide to control mosquitoes, M.W.J. GCE special issue 4-6 (2013)

[15] Yamamoto D.S., Sumitani M., Hatakeyama M., Matsuoka H., Malaria infectivity of xanthurenic acid-deficient anopheline mosquitoes produced by TALEN-mediated targeted mutagenesis, Transgenic Res. 27 (2018) 51–60 https://doi.org/10.1007/s11248-018-0057-2

[16] Rossi F., Garavaglia S., Giovenzana G.B., Arcà B., Li J., Rizzi M., Crystal structure of the Anopheles gambiae 3-hydroxykynurenine transaminase. Proc. Natl. Acad. Sci. USA 103 (2006) 5711-5716 https://doi.org/10.1073/pnas.0510233103

[17] da Silva-Alves D.C., dos Anjos J.V., Cavalcante N.N., Santos G.K., Navarro D.M., Srivastava R.M., Larvicidal isoxazoles: Synthesis and their effective susceptibility towards Aedes aegypti larvae, Bioorg. Med. Chem. 21 (2013) 940-947 https://doi.org/10.1016/j.bmcl.2010.09.055

[18] Oliveira V.S., Pimenteira C., da Silva-Alves D.C.B., Leal L.L.L., Neves-Filho R.A.W., Navarro D.M.A.F., Santos G.K.N., Dutra K.A., dos Anjos J.V., Soares T.A., The enzyme 3-hydroxykynurenine transaminase as potential target for 1,2,4-oxadiazoles with larvicide activity against the dengue vector *Aedes aegypti*, Bioorg. Med. Chem. 21 (2013) 6996-7003 http://dx.doi.org/10.1016/j.bmc.2013.09.020

[19] Sadok I., Gamian A., Staniszewska M.M., Chromatographic analysis of tryptophan metabolites, J. Sep. Sci. 40 (2017) 3020-3045 https://doi.org/10.1002/jssc.201700184

[20] Zhu W., Stevens A.P., Dettmer K., Gottfried E., Hoves S., Kreutz M., Holler E., Canelas A.B., Kema I., Oefner P.J., Quantitative profiling of tryptophan metabolites in serum, urine, and cell culture supernatants by liquid chromatography-tandem mass spectrometry, Anal. Bioanal. Chem. 401 (2011) 3249-3261 https://doi.org/10.1007/s00216-011-5436-y

[21] Du T.T., Cui T., Qiu H.M., Wang N.R., Huang D., Jiang X.H., Simultaneous determination of tryptophan, kynurenine, kynurenic acid and two monoamines in rat plasma by HPLC-ECD/DAD, J. Pharm. Biomed. Anal., 158 (2018) 8-14 https://doi.org/10.1016/j.jpba.2018.05.032

[22] Li J., Li G., Identification of 3-hydroxykynurenine and xanthurenic acid and quantitation of 3-hydroxykynurenine transaminase activity using HPLC with electrochemical detection, J. Liq. Chromatogr. Relat. Technol. 21 (1998) 1511-1525 https://doi.org/10.1080/10826079808000531

[23] Rossi F., Lombardo F., Paglino A., Cassani C., Miglio G., Arca` B., Rizzi M., Identification and biochemical characterization of the *Anopheles gambiae* 3-hydroxykynurenine transaminase, FEBS J. 272 (2005) 5653-5662. https://doi.org/10.1111/j.1742-4658.2005.04961.x

[24] Han Q., Fang J., Li J. 3-Hydroxykynurenine transaminase identity with alanine glyoxylate transaminase, A probable detoxification protein in Aedes aegypti, J. Biol. Chem. 272 (2005) 5653-5662 https://doi.org/10.1074/jbc.M201202200

[25] Butenandt A., Hallmann G., Beckmann R., Synthesis of 3-hydroxykinurenine, Chem. Ber. 90 (1957) 1120-1124

[26] Mizdrak J., Hains P.G., Kalinowski D., Truscott R.J.W., Davies M.J., Jamie J.F., Novel human lens metabolites from normal and cataractous human lenses, Tetrahedron 63 (2007) 4990-4999 https://doi.org/10.1167/iovs.13-13464

[27] Vazquez S., Garner B., Sheil M.M., Truscott R.J., Characterisation of the major autoxidation products of 3-hydroxykynurenine under physiological conditions, Free Radic. Res. 32;1 (2000) 11-23

Figures and tables

Figure 1 The kynurenine pathway in the *Anopheles gambiae* mosquito. Enzymes involved are abbreviated as follows: TDO, tryptophan 2,3-dioxygenase; KMO, Kynurenine monooxygenase; KAT, Kynurenine aminotransferase; 3-HKT, 3-hydroxykynurenine transaminase

Figure 1

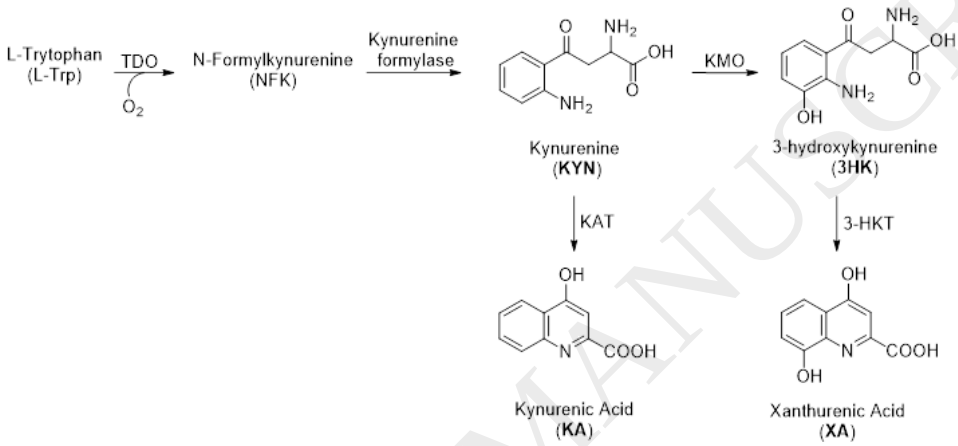

Figure 2 a. Chemical structures of **INI** and **3-OH-INI** inhibitors; **b.** Scheme of **3-OH-INI** synthesis

Figure 2

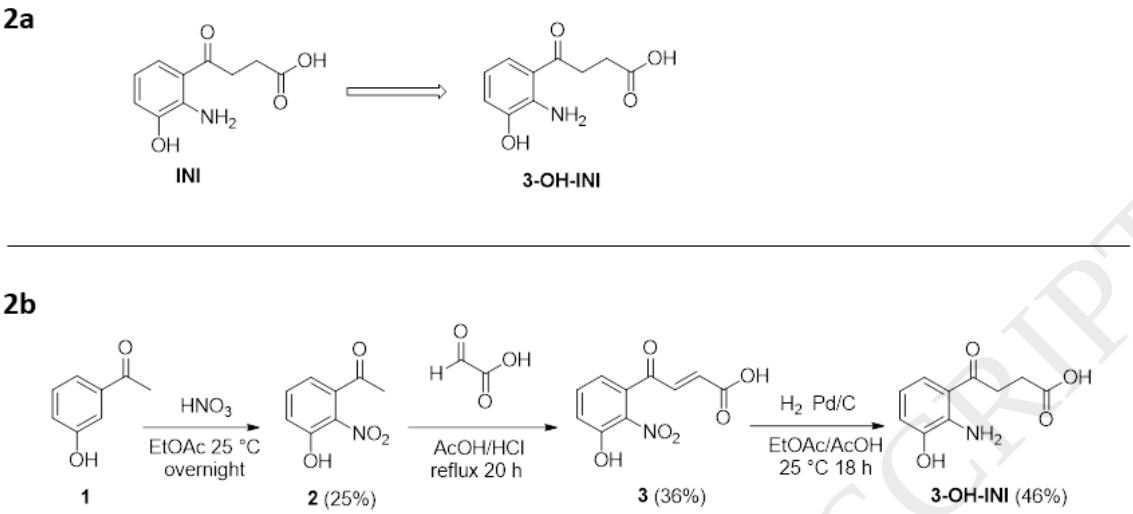

Figure 3 Representative extracted ion chromatograms corresponding to the PLP-dependent transamination of L-KYN to KA catalysed by the recombinant form of *Ag*-HKT in the presence of IS

Figure 3

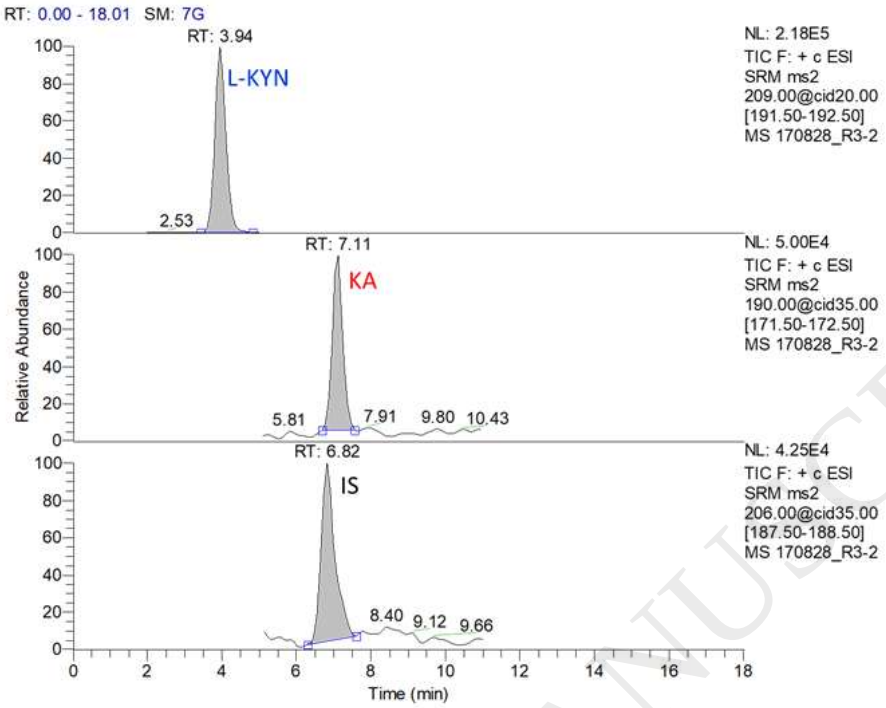

Figure 4 Kinetic study of **3-OH-INI** mechanism of *Ag*-HKT inhibition. Overlaid Lineweaver-Burk reciprocal plots of **3-OH-INI** compound

Figure 4

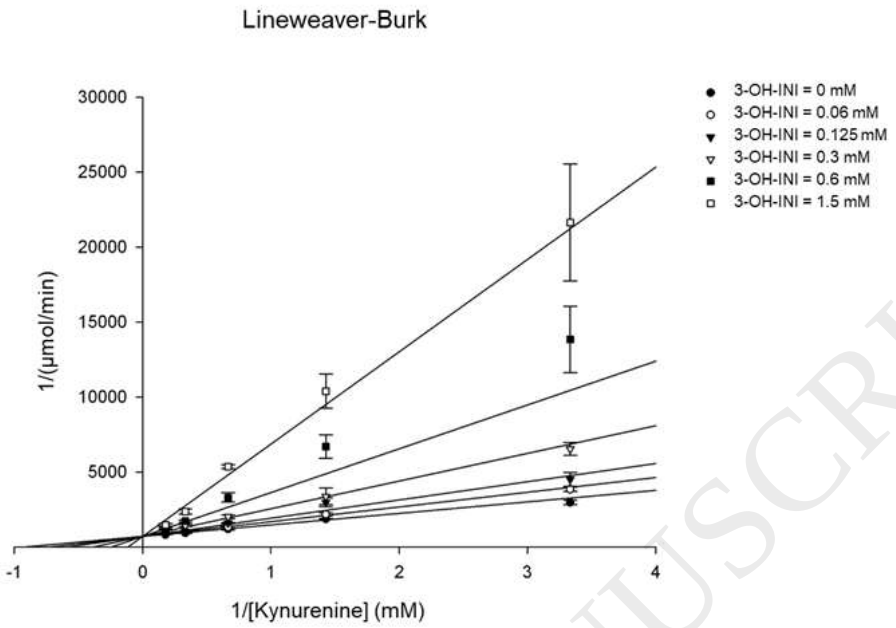

TABLE

Table 1 Accuracy and precision data of KA using internal standard

Analyte	**Intra-serie**									**Inter-series**		
KA	**Series 1**			**Series 2**			**Series 3**					
[µM]	**Mean**	**Accuracy**	**RSD**	**Mean**	**Accuracy**	**RSD**	**Mean**	**Accuracy**	**RSD**	**Mean**	**Accuracy**	**RSD**
0,25	0,28	111,21	13,34	0,27	109,38	7,87	0,27	109,22	13,96	0,27	109,94	10,94
1,0	0,88	88,21	6,73	0,98	97,97	5,31	0,88	87,76	4,67	0,90	90,03	9,24
10	9,05	90,50	4,45	9,04	90,36	7,21	9,48	94,84	2,22	9,19	91,90	5,10
50	47,35	94,70	8,88	51,32	102,65	3,23	49,61	99,22	2,39	49,43	98,86	6,02
Mean = mean of calculated concentration (µM); Accuracy = accuracy %; RSD = relative standard deviation (%)												